J. Fluid Mech. (1985), *vol.* 159, *pp.* 487–501
Printed in Great Britain

On the fluid dynamics of the aortic valve

By F. K. WIPPERMANN
Technische Hochschule Darmstadt, Fachbereich Mechanik, D-6100 Darmstadt, FRG

(Received 18 February 1985)

An aortic-valve model is developed, having a quadratic cross-section, two rigid cusps and two wedge-shaped aortic sinuses. The flow through this valve is assumed to be one-dimensional, just as the flow behind the cusps should be one-dimensional. The resulting model equations are two nonlinear ordinary differential equations of second order for the valve opening area as a function of time in two different ranges.

This model allows the size of the aortic sinus to be varied; it also permits a computation of the pressure at both sides of the cusps (unlike previous models of this kind, which consider the flow behind the cusps as stagnant). The computed valve motion due to this pressure difference is in good agreement with experimental results, although no vortex with circular streamlines is postulated in the aortic sinuses. Obviously such vortices trapped in the sinuses are not important for the valve closure, which is controlled solely by the flow deceleration.

1. Introduction

The aortic valve controls the flow of oxygenated blood from the left ventricle into the aorta. It is a non-return valve, which works very efficiently.

During the first part of the ventricular systole the three cusps in the valve open promptly with the rapidly ejected blood. However, in the second part of the systole the cusps are already driven towards their closure position, even though the flow is still forward; 75–80% of the closure is already completed before the aortic flow becomes zero. Only a very small reversed flow of about 2–4% of the total forward flow then completes the closure by sealing the valve.

In the last fifteen years, beginning with the pioneering work by Bellhouse & Talbot (1969), numerous investigators have been attracted by the problem of how to explain the pressure difference across the cusp which moves the cusp into the forward flow.

One explanation goes back to Leonardo da Vinci (1513). He found in his anatomical studies three marked dilatations of the root of the aorta, called aortic sinuses or sinuses of Valsalva, one sinus behind each cusp of the valve. Leonardo predicted that vortices would be formed in the sinuses and that they would feature in the control mechanism of the valve.

Almost four hundred years later an alternative explanation of valve closure was given by two physiologists (Henderson & Johnson 1912). According to these authors, the deceleration of the aortic flow is mainly responsible for the cusp's movement into the forward flow; they themselves called it the 'breaking of the jet'.

Leonardo's prediction stimulated a number of experiments with physical models to study the dynamics of natural heart valves, aortic as well as mitral ones (e.g. Bellhouse 1969, 1972; Bellhouse & Talbot 1969; van Steenhoven & van Dongen 1979; Lee & Talbot 1979; van Steenhoven *et al.* 1980). Most of these authors have also put their experimental findings into a theory; see for instance Bellhouse & Talbot (1969),

who model the fluid motion in the sinus for the peak-flow period with the aid of a modified Hill vortex.

It has been concluded from the earliest of these experiments and theories (e.g. Bellhouse 1969) that the fluid vortex trapped within each sinus plays an essential role in the early phase of valve closure (Hwang 1977), that the vortices help to position the cusps at peak systole and that the vortices contribute to the prevention of jet formation from the narrowing valve opening.

However, an explanation of valve closure that relies solely on the thrust of vortices trapped in the sinuses is incomplete (Bellhouse 1980) – the flow deceleration is needed too. Lee & Talbot (1979) state that the adverse pressure gradient related to the deceleration of the valve flow is the primary mechanism for efficient valve closure. Also, van Steenhoven & van Dongen (1979) concluded from their experiments that a vortex trapped in the sinus does not essentially affect the mechanism of valve operation; however, it must be noted that the flow deceleration in their experiments starts from the steady state.

In this paper an attempt is made to show that the closing of the aortic valve will function correctly also without any control by vortices trapped in the sinuses and without additional thrust by such vortices to aid closure in the latter part of systole. For this purpose the fluid in the sinuses is not considered stagnant as in the above-mentioned earlier theories, but the pressure at the sinus side of the cusps is computed from displacement of fluid in the valve opening and replacement during valve closure. Moreover, the use of a one-dimensional model will prohibit the formation of a vortex with circular streamlines in the sinuses.

2. Short description of the natural aortic valve

The natural aortic valve consists of three equal-sized crescent-shaped (or semilunar) cusps, each of which is supported at its base by a near-cylindrical cuff, the human aortic root having an inside diameter of approximately 25 mm. The cusps are non-muscular and 0.2–0.4 mm thick, they are reinforced with collagen strands running from commissure to commissure. The cusps are passive devices which 'float' in the blood stream.

In the closed phase (ventricular diastole) the free margins of the leaflets come together and seal each other when the left ventricular pressure falls below aortic pressure; then the cusps have to support a pressure difference of about 100 mmHg (13.3 kPa). The bottom surface angle α (see figure 1, left-hand side) is about 20° in the closed phase (Swanson & Clark 1974).

As Davila (1961) showed photographically, the aortic leaflets do not actually open fully in systole because of the enlargement of the circular orifice by aortic distension. The opened leaflets lie as three cords within the circle, forming a triangular orifice.

However, Bellhouse & Talbot (1969) showed in an experiment with a rigid-walled model that aortic leaflets do open fully during systole and provide almost no obstacle to the blood flow. Bellhouse (1969) concluded from his experiments (for a steady flow) that the downstream edges of the cusps can project into the sinus cavities by 9.1 % of the aortic radius.

Three permanent dilatations of the aorta, matching each cusp, are called aortic sinuses or sinuses of Valsalva after the Italian anatomist who published in 1740 the first anatomical account of the aortic sinuses. The size and shape of the sinuses can be seen in the left part of figure 1, where all lengths are non-dimensionalized by the radius r_0 of the aorta at its root.

From two of these three sinuses spring the coronary arteries, which supply

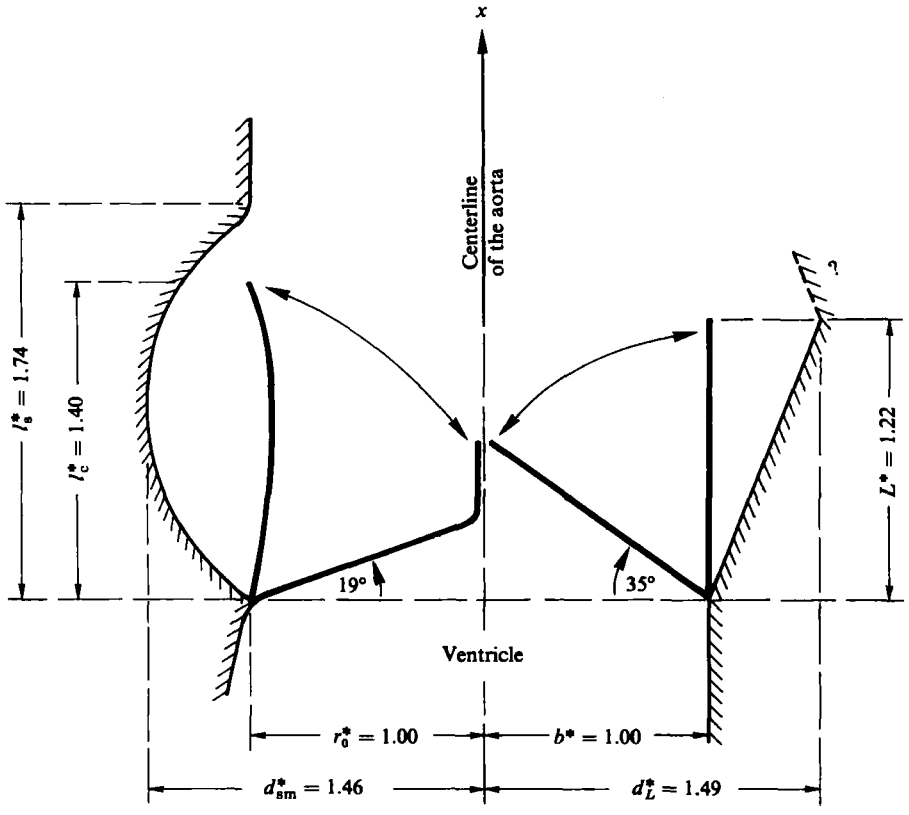

FIGURE 1. The size of the aortic valve (cross-sectional). Left-hand side: natural valve. Right-hand side: model valve. The asterisk indicates non-dimensionalization by r_0 or b.

oxygenated blood to the heart muscle. It may be one function of the vortices within the sinuses to avoid a sealing of these orifices by the leaflets protruding into the sinus cavities, when the valve is fully open.

The aorta itself and the sinuses vary in diameter, and the leaflets vary in length, as the pressure varies during a cardiac cycle (see Swanson & Clark 1974). However, these variations are very small indeed and can be neglected in the following considerations.

3. The valve model

The model aorta has a quadratic transverse section, the size of which is $A_0 = 4b^2$ (see figures 1 and 2).

Instead of three cusps in the natural valve, there are only two rectangular ones in the model; they are trap-like, each one being supported by a rule-joint on the side of the aorta opposite to the other trap. These model cusps are assumed to be rigid and to have zero mass. The size of such a 'cusp' equals $2bL$. The cusp length L determines the bottom angle α_{CL} (see figure 1, right-hand side). This should correspond roughly to the angle that is made between the cross-sectional plane and the plane of the cusp (in closed position), i.e. about 35°. The corresponding length L in the natural valve will be larger by about 15% when the cusp is stretched. The notation $b/L = k$ is frequently used.

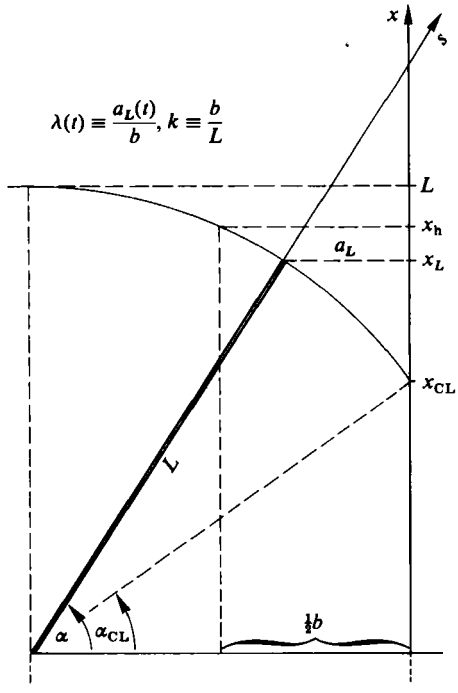

FIGURE 2. Symbols used in the valve model.

The model is a one-dimensional one: the only coordinate is along the x-axis of the aorta. The flow has a u-component only, i.e. it is considered to be homogeneous across the valve. This may be justified at least partially by the findings of other authors, that the flow is laminar, the profile is flat and does not show a central jet (Bellhouse & Talbot 1969; Bellhouse 1980).

The cross-sectional area of the valve between the cusps is

$$A(x,t) = A_0 \left\{1-[1-\lambda(t)]\frac{x}{x_L}\right\}, \tag{1}$$

where

$$x_L = L\{1-k^2[1-\lambda(t)]^2\}^{\frac{1}{2}} \tag{2}$$

is the x-coordinate of the moving distal margin of the cusp. The meaning of the symbols can be seen from figure 2.

$x_L = L$ when the valve is fully open and $x_L = x_{CL}$ is the closed position:

$$x_{CL} = L\{1-k^2\}^{\frac{1}{2}}, \tag{3}$$

i.e. x_L ranges between x_{CL} and L.

$$\lambda(t) = \frac{a_L(t)}{b} = \frac{A(x_L,t)}{A_0} \tag{4}$$

is the single degree of freedom of this model valve; λ is called the (relative) valve-opening area.

If $\lambda = 0.5$, $x_L = x_h$, where

$$x_h = L\{1-\tfrac{1}{4}k^2\}^{\frac{1}{2}}, \tag{5}$$

an expression that is needed later on.

The other existing theories differ primarily in the assumption about the fluid behind the valve leaflets. Either the flow over there is modelled by a Hill spherical vortex and matched to the main stream (e.g. Bellhouse & Talbot 1969) or the pressure in

the aortic sinuses is assumed to be uniform and equal to the pressure at the cusp margins.

In the present model the fluid behind the cusps is displaced in valve opening and moved backward in valve closing. This motion (assumed to be one-dimensional too) is computed from the continuity condition and allows the pressure $p(s)$ along the reverse side of the cusp to be obtained.

Therefore one has to distinguish the flow inside the cusps (suffix i) from the flow behind the cusps, i.e. on their sinus side (suffix a); the same is applicable to the sectional area $A(x,t)$:

$$u_\mathrm{i} A_\mathrm{i} + u_\mathrm{a}[(A_0 - A_\mathrm{i}) + A_\mathrm{s}] = u_0 A_0. \tag{6}$$

A_s is the sectional area of the sinus of Valsalva; its maximum $A_\mathrm{s}(L)$ is determined by the semicircles drawn from the centre of each side of a triangle inscribed into the circular aorta. One finds for $A_\mathrm{s}(L)$

$$\frac{A_\mathrm{s}(L)}{A_0} = \tfrac{3}{2}\left\{\sin^2 \tfrac{1}{6}\pi + \frac{1}{\pi}\sin \tfrac{1}{3}\pi\right\} - 1 = 0.539.$$

The assumption of a wedge-shaped aortic sinus means that this area increases linearly with increasing distance x from the valve orifice:

$$A_\mathrm{s}(x) = 0.539 m \frac{x}{L} A_0 \quad (x \leqslant L). \tag{7}$$

Of course, A_s has its maximum at $x = L$, but not at $x \approx \frac{2}{3}L$ as in nature (see figure 1, left-hand side). The shape and size of the sinus for $x > L$ do not matter in the case of such a one-dimensional model. The factor m in (7) allows for a variation of the size of the aortic sinus; $m = 1$ gives the natural maximal size at $x = L$.

Undoubtedly there are several other more sophisticated models having fewer restrictions (e.g. Peskin 1972; McCracken & Peskin 1980; Hung & Schuessler 1977), but these seem to be less suitable for the purpose of this paper.

4. The basic equations

We start with almost the same set of equations as applied by Peskin (1982) in his review paper when he describes the motion of valves with a single degree of freedom. The equations are

$$A_\mathrm{i}(x,t) = A_0\left\{1 - [1-\lambda(t)]\frac{x}{x_L(t)}\right\} \quad (0 \leqslant x \leqslant x_L), \tag{8a}$$

$$A_\mathrm{a}(x,t) = A_0\left\{[1-\lambda(t)]\frac{x}{x_L(t)} + 0.54m\frac{x}{L}\right\}, \tag{8b}$$

$$\frac{\partial}{\partial t}A_\mathrm{i} + \frac{\partial}{\partial x}(A_\mathrm{i} u_\mathrm{i}) = 0, \quad \frac{\partial}{\partial t}A_\mathrm{a} + \frac{\partial}{\partial x}(A_\mathrm{a} u_\mathrm{a}) = 0, \tag{9a,b}$$

$$\rho\left(\frac{\partial}{\partial t}u_\mathrm{i} + u_\mathrm{i}\frac{\partial}{\partial x}u_\mathrm{i}\right) + \frac{\partial}{\partial x}p_\mathrm{i} = 0. \tag{10a}$$

$$\rho\left(\frac{\partial}{\partial t}u_\mathrm{a} + u_\mathrm{a}\frac{\partial}{\partial x}u_\mathrm{a}\right) + \frac{\partial}{\partial x}p_\mathrm{a} = 0, \tag{10b}$$

$$\int_0^L s\{p_\mathrm{a}(s,t) - p_\mathrm{i}(s,t)\}\,\mathrm{d}s = 0, \quad s = L\frac{x}{x_L}. \tag{11}$$

In these equations u is the axial velocity, p is the pressure, A is the cross-sectional area of the valve, L is the length of the cusps and $\lambda(t)$ is the single degree of freedom. This $\lambda(t)$ is the (relative) valve opening area as defined in (4). s is the coordinate along the cusp (see figure 2) and m is a factor taking account of enlargement or reduction of the size of the aortic sinus.

Equations $(8a, b)$ are an expression of the geometry of the planar model (see (1), (6), (7)), whereas $(9a)$, $(10a)$ and $(9b)$, $(10b)$ are the one-dimensional forms of the incompressible Euler equations. The cusps are assumed to have zero mass, thus the torque acting on a cusp must vanish. That is expressed by (11). Other authors (e.g. van Steenhoven & van Dongen 1979; Peskin 1982) postulate that only the acting forces have to balance; this causes slight differences in the results.

With (2), $(8a)$–(11) a set of eight nonlinear equations is available for the eight variables A_a, A_i, u_a, u_i, p_a, p_i, x_L and λ; they all depend on x and t, except for x_L and λ, which depend on t only. This set of equations can be solved only by a simultaneous numerical integration.

However, when allowance is made for some approximative simplifications, seven of the eight variables can be eliminated, yielding a single equation for the valve-opening area λ; this will be an ordinary differential equation for $\lambda(t)$ in terms of the velocity at the orifice $u_0(t) = u(0, t)$.

The abovementioned approximations imply that such a differential equation can be derived only for a certain rather short period of time, e.g. for times when $\lambda \approx 1$. Here the derivation should be restricted to three such short periods, namely to times when $\lambda \approx 1$, $\lambda \approx 0.5$ and $\lambda \approx 0$. However, afterwards the three differential equations thus obtained, valid only for three special times, will be combined again by a kind of matching in order to have an equation also for the intermediate times when $1 > \lambda > 0.5$ or $0.5 > \lambda > 0$ respectively. The first step follows partly from the work of van Steenhoven & van Dongen (1979), who carried out the derivation approximately for times when $\lambda \approx 1$. Owing to these approximations, the derived differential equation remains a linear one.

These approximations can be achieved by setting $\lambda = \lambda_* + \epsilon\lambda_1$ ($\lambda_* = 1$, 0.5 or 0) and then retaining only terms up to first order in ϵ. The linearizations thus achieved are as in table 1.

	$\lambda_* = 1$	$\lambda_* = \frac{1}{2}$	$\lambda_* = 0$
λ^2	$2\lambda - 1$	$\lambda - \frac{1}{4}$	0
$(1-\lambda)^2$	0	$\frac{3}{4} - \lambda$	$1 - 2\lambda$
$(1-\lambda)^3$	0	$\frac{1}{2} - \frac{3}{4}\lambda$	$1 - 3\lambda$
$\lambda \dfrac{d\lambda}{dt}$	$\dfrac{d\lambda}{dt}$	$\dfrac{1}{2}\dfrac{d\lambda}{dt}$	0
$(1-\lambda)\dfrac{d\lambda}{dt}$	0	$\dfrac{1}{2}\dfrac{d\lambda}{dt}$	$\dfrac{d\lambda}{dt}$
$(1-\lambda)^2\dfrac{d\lambda}{dt}$	0	$\dfrac{1}{4}\dfrac{d\lambda}{dt}$	$\dfrac{d\lambda}{dt}$
$x_L(\lambda_*)$	L	$x_h = L(1-\frac{1}{4}k^2)^{\frac{1}{2}}$	$x_{CL} = L(1-k^2)^{\frac{1}{2}}$

TABLE 1

5.1. *Derivation of the λ-equation for times when λ ≈ 1*

By substituting (8*a*) into (9*a*) and (8*b*) into (9*b*) and integrating once in x, one gets expressions for $u_i(x,t)$ or $u_a(x,t)$ respectively, both in terms of $\lambda(t)$:

$$u_i(x,t) = u_0 + (1-\lambda)\,u_0\,\frac{x}{L} - \frac{d\lambda}{dt}\,\frac{L}{2}\,\frac{x^2}{L^2} \quad (0 \leqslant x \leqslant x_L \approx L), \tag{12a}$$

$$u_a(x,t) = \frac{d\lambda}{dt}\,\frac{2L}{N}\,\frac{x}{L}, \quad N = 4(0.52m + 1 - \lambda). \tag{12b}$$

Now (12*a*) can be substituted into (10*a*) and (12*b*) into (10*b*) respectively, and on integrating once again in x one obtains expressions for $p_i(x,t)$ and $p_a(x,t)$ respectively, in terms of $\lambda(t)$:

$$\frac{1}{\rho}\,p_i(x,t) - \frac{1}{\rho}\,p_i(0,t) = -\left\{(1-\lambda)\,u_0^2 + \frac{d}{dt}\,u_0 L\right\}\frac{x}{L} + \left\{\frac{d\lambda}{dt}\,u_0 L - \tfrac{1}{2}(1-\lambda)\,\frac{d}{dt}\,u_0 L\right\}\frac{x^2}{L^2} + \frac{1}{6}\,\frac{d^2\lambda}{dt^2}\,L^2\,\frac{x^3}{L^3}, \tag{13a}$$

$$\frac{1}{\rho}\,p_a(x,t) = \frac{1}{\rho}\,p_i(L,t) + \frac{d^2\lambda}{dt^2}\,\frac{L^2}{N}\left(1 - \frac{x^2}{L^2}\right). \tag{13b}$$

The boundary condition for the last integration is $u_a(0,t) = 0$. Of course, the condition $p_a(x_L,t) = p_i(x_L,t)$ must be taken into account.

For $N \to \infty$ (i.e. $m \to \infty$, the size of the aortic sinus approaches infinity)

$$p_a(x) = p_i(L) = \text{const.},$$

which is the assumption made by several authors for the pressure at the sinus side of the cusp.

Substituting (13*a*, *b*) into (11) yields the following ordinary differential equation:

$$\frac{d^2\lambda}{dt^2} + f_1\,\frac{d\lambda}{dt} + f_2\,\lambda = f_3, \tag{14}$$

where

$$f_1 = \frac{u_0}{L}\,5\,\frac{1}{M_1(m)},$$

$$f_2 = \frac{u_0^2}{L^2}\,\frac{10}{3}\,\frac{1}{M_1(m)} + \frac{1}{L}\,\frac{du_0}{dt}\,\frac{5}{2}\,\frac{1}{M_1(m)}\left\{1 + \frac{16}{3}\,\frac{1}{2.16m}\right\},$$

$$f_3 = \frac{u_0^2}{L^2}\,\frac{10}{3}\,\frac{1}{M_1(m)} + \frac{1}{L}\,\frac{d\lambda}{dt}\,\frac{1}{M_1(m)}\left\{\frac{5}{2}\left(1 + \frac{16}{3}\,\frac{1}{2.16m}\right) + \frac{10}{3}\right\},$$

$$M_1 = 1 + \frac{5}{2.16m}.$$

Equation (14) is very similar to that obtained by van Steenhoven & van Dongen (1979) or by Peskin (1982); their assumption $p_a(x,t) = p_i(x_L,t) \approx p_i(L,t)$ requires $m \to \infty$ or $M_1 = 1$. With that, (14) reads

$$\frac{d^2\lambda}{dt^2} + \frac{d\lambda}{dt}\,\frac{u_0}{L}\,c_1 - (1-\lambda)\left\{\frac{u_0^2}{L^2}\,c_2 + \frac{1}{L}\,\frac{d\lambda}{dt}\,c_3\right\} = \frac{1}{L}\,\frac{du_0}{dt}\,c_4.$$

The coefficients $c_1, \ldots, c_4$ in this equation should be compared with those in the equations of van Steenhoven & van Dongen and Peskin; see table 2.

	c_1	c_2	c_3	c_4
Equation (14), $m\to\infty$	5	$\frac{10}{3}$	$\frac{5}{2}$	$\frac{10}{3}$
van Steenhoven & van Dongen	$\frac{16}{3}$	4	$\frac{8}{3}$	4
Peskin	$\frac{16}{3}$	4	$\frac{8}{3}$	2

TABLE 2

The slight differences in the coefficients $c_1, \ldots, c_4$ are due to the use of the torque in (11) instead of the forces as were used by van Steenhoven & van Dongen as well as by Peskin. The difference in c_4 between the latter two is explained by the different model geometry (planar model in van Steenhoven & van Dongen, a truncated cone model in Peskin, for which the valve-opening area $A_L/A_0 = \lambda^2$). Nevertheless, one gets the impression that the type of equation is more or less invariant for modifications of the model. Computations with a three-cusp model and a hexagonal model with six cusps (both with a star-shaped cross-sectional area of the valve) yield the same type of equation.

For a non-pulsatile flow the valve has a stable equilibrium configuration given by $\lambda = 1$. When $\mathrm{d}u_0/\mathrm{d}t < 0$ the cusps are driven towards the closing position even though u_0 is still positive. This shows the importance of deceleration in closing the valve.

5.2. *Derivation of the λ-equation for times when $\lambda \approx 0.5$*

The derivation is analogous to that in §5.1. By substituting (8*a*) into (9*a*) and (8*b*) into (9*b*) and integrating once in x (using the linearizations in λ for $\lambda_* = 0.5$) one obtains again the expressions for $u_i(x,t)$ and $u_a(x,t)$, both in terms of $\lambda(t)$:

$$u_i(x,t) = u_0 + (1-\lambda)\,u_0\frac{x}{x_h} - \frac{\mathrm{d}\lambda}{\mathrm{d}t}\frac{x_h}{2}\left(\frac{x}{x_h}\right)^2 - \frac{\mathrm{d}\lambda}{\mathrm{d}t}\frac{x_h}{4}\left(\frac{x}{x_h}\right)^3 \quad (0 \leqslant x \leqslant x_L \approx x_h), \tag{15a}$$

$$u_a(x,t) = \frac{\mathrm{d}\lambda}{\mathrm{d}t}\frac{2x_h}{N}\frac{x}{x_h}. \tag{15b}$$

After this, (15*a*) is substituted into (10*a*) and (15*b*) into (10*b*). Integrating once again in x, one obtains expressions for $p_i(x,t)$ and $p_a(x,t)$ respectively, in terms of $\lambda(t)$:

$$\begin{aligned}\frac{1}{\rho}p_i(x,t) - \frac{1}{\rho}p_i(0,t) = &-\left\{(1-\lambda)\,u_0^2 + \frac{\mathrm{d}u_0}{\mathrm{d}t}x_h\right\}\frac{x}{x_h}\\ &+\left\{\frac{\mathrm{d}\lambda}{\mathrm{d}t}u_0 x_h - (1-\lambda)\frac{\mathrm{d}u_0}{\mathrm{d}t}\frac{x_h}{2} - (\tfrac{3}{4}-\lambda)\frac{u_0^2}{2}\right\}\left(\frac{x}{x_h}\right)^2\\ &+\left\{\frac{\mathrm{d}\lambda}{\mathrm{d}t}u_0\frac{x_h}{2} + \frac{\mathrm{d}^2\lambda}{\mathrm{d}t^2}\frac{x_h^2}{6}\right\}\left(\frac{x}{x_h}\right)^3\\ &+\left\{\frac{\mathrm{d}\lambda}{\mathrm{d}t}u_0\frac{x_h}{8} + \frac{\mathrm{d}^2\lambda}{\mathrm{d}t^2}\frac{x_h^2}{16}\right\}\left(\frac{x}{x_h}\right)^4,\end{aligned} \tag{16a}$$

$$\frac{1}{\rho}p_a(x,t) = \frac{1}{\rho}p_i(x_h,t) + \frac{\mathrm{d}^2\lambda}{\mathrm{d}t^2}\frac{x_h^2}{N_h}\left\{1-\left(\frac{x}{x_h}\right)^2\right\}. \tag{16b}$$

The boundary conditions at $x = 0$ for the integrations are $u_i = u_0$ and $u_a = 0$. Of course, the condition $p_a(x_L,t) = p_i(x_L,t)$ is also used. $N_h = 4(0.52mx_h/L + 1 - \lambda)$, where N is defined in (12*b*).

Again, for $N_h \to \infty$ (i.e. $m \to \infty$, the size of the aortic sinus approaches infinity) the pressure at the sinus side of the cusps is uniform and equals the pressure at the distal end of the cusps.

Substituting (16a, b) into (11) yields the following differential equation:

$$\frac{\mathrm{d}^2\lambda}{\mathrm{d}t^2} + g_1 \frac{\mathrm{d}\lambda}{\mathrm{d}t} + g_2 \lambda = g_3, \tag{17}$$

where

$$g_1 = \frac{u_0}{L} \tfrac{212}{89}(1-\tfrac{1}{4}k^2)^{-\frac{1}{2}} \frac{1}{M_2(k,m)} \{2.16(1-\tfrac{1}{4}k^2)^{\frac{1}{2}} m + 2\},$$

$$g_2 = \frac{u_0^2}{L^2} \tfrac{85}{89}(\tfrac{28}{17} - k^2)(1-\tfrac{5}{4}k^2+\tfrac{1}{4}k^4)^{-1} \frac{1}{M_2(k,m)} \{2.16(1-\tfrac{1}{4}k^2)^{\frac{1}{2}} m + \tfrac{78}{17}(\tfrac{50}{39} - k^2)(\tfrac{28}{17} - k^2)^{-1}\}$$

$$+ \frac{1}{L}\frac{\mathrm{d}u_0}{\mathrm{d}t} \tfrac{50}{89}(\tfrac{6}{5} + k^2)(1-\tfrac{1}{4}k^2)^{-\frac{1}{2}}(1-k^2)^{-1}$$

$$\times \frac{1}{M_2(k,m)} \{2.16(1-\tfrac{1}{4}k^2)^{\frac{1}{2}} m + \tfrac{34}{5}(\tfrac{28}{17} - k^2)(\tfrac{6}{5} + k^2)^{-1}\},$$

$$g_3 = \frac{u_0^2}{L^2} \tfrac{195}{89}(\tfrac{50}{39} - k^2)(1-\tfrac{5}{4}k^2+\tfrac{1}{4}k^4)^{-1} \frac{1}{M_2(k,m)} \{2.16(1-\tfrac{1}{4}k^2)^{\frac{1}{2}} m + \tfrac{56}{39}(\tfrac{18}{7} - k^2)(\tfrac{50}{39} - k^2)^{-1}\}$$

$$+ \frac{1}{L}\frac{\mathrm{d}u_0}{\mathrm{d}t} \tfrac{85}{89}(\tfrac{48}{17} - k^2)(1-\tfrac{1}{4}k^2)^{-\frac{1}{2}}(1-k^2)^{-1}$$

$$\times \frac{1}{M_2(k,m)} \{2.16(1-\tfrac{1}{4}k^2)^{\frac{1}{2}} m + \tfrac{78}{17}(\tfrac{50}{39} - k^2)(\tfrac{48}{17} - k^2)^{-1}\},$$

$$M_2(k,m) = 2.16(1-\tfrac{1}{4}k^2)^{\frac{1}{2}} m + \tfrac{538}{89}.$$

Throughout the calculations in this subsection $\lambda = 0.5 + \epsilon\lambda_1$, and only terms up to first order in ϵ are retained, i.e. the linearizations in λ according to table 1, $\lambda_* = 0.5$, are used.

5.3. *Derivation of the λ-equation for times when $\lambda \approx 0$*

By substituting (8a) into (9a) and integrating once in x, one obtains the velocity u_i in terms of $\lambda(t)$:

$$u_i(x,t) = 2u_0 - \frac{L}{(1-k^2)^{\frac{3}{2}}} \frac{\mathrm{d}\lambda}{\mathrm{d}t} \left(\frac{x}{L}\right)^2, \tag{18}$$

where the linearizations in λ for $\lambda_* = 0$ (see table 1) are used, and $1-\lambda \approx 1$ is taken in the denominator; also a mean value of x ($0 \leqslant x \leqslant x_L \approx x_{CL}$), $\bar{x} \to \frac{1}{2}x_L$, has been used in the denominator. This expression differs considerably from that obtained by Lee & Talbot (1979), who made the assumption $\partial u_i/\partial x = 0$ for $\lambda \approx 0$; they justified this by an indirect consideration of the frictional effects. These authors obtained a first-order differential equation for λ instead of the second-order differential equation (20). One substitutes (18) into (10a), integrates once in x and obtains the pressure $p_i(x,t)$ in terms of $\lambda(t)$:

$$\frac{1}{\rho} p_i(x,t) = \frac{1}{\rho} p_i(0,t) - \tfrac{3}{2}u_0^2 - 2L\frac{\mathrm{d}u_0}{\mathrm{d}t}\frac{x}{L} + \frac{2Lu_0}{(1-k^2)^{\frac{3}{2}}}\frac{\mathrm{d}\lambda}{\mathrm{d}t}\left(\frac{x}{L}\right)^2 + \frac{L^2}{3(1-k^2)^{\frac{3}{2}}}\frac{\mathrm{d}^2\lambda}{\mathrm{d}t^2}\left(\frac{x}{L}\right)^3. \tag{19a}$$

For $\lambda \approx 0$, i.e. for the early opening or the final closing, the motion of the cusps is almost independent of the size of the aortic sinus. Therefore the pressure p_a on the

back of the cusp can be assumed to be uniform and equal to the pressure at the cusp's margin:

$$p_a(x,t) = p_i(x_L,t) \approx p_i(x_{CL},t). \tag{19b}$$

Now (19a, b) are substituted into (11); this yields the following ordinary differential equation:

$$\frac{d^2\lambda}{dt^2} + h_1 \frac{d\lambda}{dt} + h_2 \lambda = h_3, \tag{20}$$

$$h_1 = \frac{u_0}{L} 5(1-k^2)^{-\frac{1}{2}},$$

$$h_2 = 0,$$

$$h_3 = \frac{1}{L} \frac{du_0}{dt} \tfrac{10}{3}(1-k^2)^{\frac{1}{2}}.$$

5.4. *The final differential equation for* $\lambda(t)$

The three λ-equations (14), (17) and (20) obtained above are valid only for times when $\lambda \approx \lambda_*$ and λ_* has special values:

(14) for $\lambda_* = 1$ $$\frac{d^2\lambda}{dt^2} + f_1 \frac{d\lambda}{dt} + f_2 \lambda = f_3, \tag{21a}$$

(17) for $\lambda_* = 0.5$ $$\frac{d^2\lambda}{dt^2} + g_1 \frac{d\lambda}{dt} + g_2 \lambda = g_3, \tag{21b}$$

(20) for $\lambda_* = 0$ $$\frac{d^2\lambda}{dt^2} + h_1 \frac{d\lambda}{dt} + h_2 \lambda = h_3. \tag{21c}$$

Now (21a, b) are fitted together by a weighted average in order to obtain a differential equation for $\lambda(t)$ valid in the range $1 > \lambda > 0.5$; the same is done with (21b, c), giving a differential equation for $\lambda(t)$ valid in the range $0.5 > \lambda > 0$. The chosen weighting functions, depending on λ, must guarantee that for $\lambda = 1, 0.5, 0$ the equations reduce to (21a, b, c) respectively. For this purpose the f_i are multiplied by $2\lambda - 1$, the g_i by $2(1-\lambda)$ for $1 > \lambda > 0.5$ and by 2λ for $0.5 > \lambda > 0$, and the h_i are multiplied by $1 - 2\lambda$.

Of course by applying such a weighted average the equations become nonlinear again; however, a single ordinary differential equation is left instead of the set of eight coupled partial differential equations (2), (8)–(11), which are also nonlinear. An insight into the mechanism of valve motion can be gained more easily with the aid of the single equation for the valve-opening area λ than with the complete set of equations; especially because the single equation shows the way in which λ depends on L, m and $u_0(t)$.

The resulting equations are as follows:

$1 > \lambda > 0.5$

$$\frac{d^2\lambda}{dt^2} + \frac{d\lambda}{dt}\{\lambda\, 2(f_1 - g_1) + 2g_1 - f_1\} + \lambda^2\, 2(f_2 - g_2) + \lambda\, 2(g_2 + g_3 - \tfrac{1}{2}f_2 - f_3) = 2g_3 - f_3, \tag{22a}$$

$0.5 > \lambda > 0$

$$\frac{d^2\lambda}{dt^2} + \frac{d\lambda}{dt}\{\lambda\, 2(g_1 - h_1) + h_1\} + \lambda^2\, 2g_2 + \lambda\, 2(h_3 - g_3) = h_3. \tag{22b}$$

The coefficients f_1, f_2, f_3 depend on $u_0(t)$, L, m; they are given in (14). The coefficients g_1, g_2, g_3 depend on $u_0(t)$, L, m, k, and the coefficients h_1, h_2, h_3 depend on $u_0(t)$, L and k; they are given in (17) and (20) respectively.

The initial conditions are

$$\lambda = 0, \quad \frac{\mathrm{d}\lambda}{\mathrm{d}t} = 0 \quad (t = 0). \tag{23}$$

After a discretization of (22a, b) and (23), the simple Euler method is applied for numerical integration; the appropriate time step is $\Delta t = 1$ ms.

6. Discussion of the results

A numerical integration of (22a, b) with initial condition (23) has been carried out for a valve with $b = 1.10$ cm, $L = 1.34$ cm (i.e. $\alpha_0 = 35°$, $k = 0.82$, $A_0 = 4.84$ cm^2, corresponding to an inside diameter of a circular aorta of 2.48 cm) and an aortic orifice velocity $u_0(t)$ as given in figure 3 by the solid line. During a period of rapid ejection of 0.1 s this velocity increases to a peak value of 90.8 cm/s and then decreases again during the following 0.16 s; after 0.26 s the flow equals zero again.

With the following diastole of 0.60 s (including a very short period for the final valve closure by backflow) the duration of one beat is 0.86 s, or the beat rate is 70 min^{-1}. This means, with the velocity $u_0(t)$ according to figure 3, that the stroke volume $V = 5$ l min^{-1}, which are quite natural conditions in non-exercising humans.

The motion of the cusps is shown in figure 4 for three different sizes of the aortic sinus, $m = 1.\bar{6}$ (solid curve) corresponds to the natural size, $m = 0.8\bar{3}$ (dotted curve) to half the natural size, and $m = \infty$ to a size approximating infinity. As mentioned earlier, the latter case is identical with the condition $p_a(x, t) = p_i(x_L, t)$, which is used by almost all other authors for the pressure $p_a(x, t)$ at the sinus side of the cusp.

According to (7), the natural size of the sinus of Valsalva is given in the model for $m = 1$, $x = L$ with $A_s = 0.54A_0$. However, for $m = 1.\bar{6}$ this size is reached already for $x = 0.6L$, the distance from the orifice at which the natural sinus is largest.

Let us consider the natural case ($m = 1.\bar{6}$): The valve opens very fast when rapid ejection begins, the cusps are already parallel to the aortic walls ($\lambda = 1$) after 65 ms of systolic time and reach maximum opening with $\lambda = 1.08$ after 89 ms, i.e. already 11 ms before the time when u_0 is maximum. Then the cusps remain more or less in this open position until the time (100 ms) when deceleration begins; then they start closing. After 129 ms they are again parallel to the aortic walls, then they close further. At zero velocity (260 ms) the cusps have swept three-quarters shut, which is in agreement with the findings of Bellhouse & Talbot (1969) and Bellhouse (1969) for pulsatile flow.

The valve-opening area is larger than 1 for about 64 ms, with a maximum of $\lambda_{max} = 1.08$. This agrees quite well with the experimental results (steady state) of Bellhouse (1969), where the downstream edges of the cusps project into the sinus cavities for 9.1 % of the aortic radius.

If the sinus in the model has only half the size of the natural one ($m = 0.8\bar{3}$, dotted curve in figure 4) the valve opens even wider, the downstream edges of the cusps project into the sinus for about 12 % of the half-diameter b. Although the cusps begin closing already after 82 ms of systolic time; the valve remains 44 % open when the orifice velocity is zero again, which is not realistic.

In the case $m \to \infty$ the time of maximum valve opening ($\lambda = 1.02$) coincides with the time of peak velocity u_0; however, in the second phase of systole the valve closes too fast; the open area at the time 260 ms ($u_0 = 0$) is $\lambda = 0.03$ only, which is quite unrealistic.

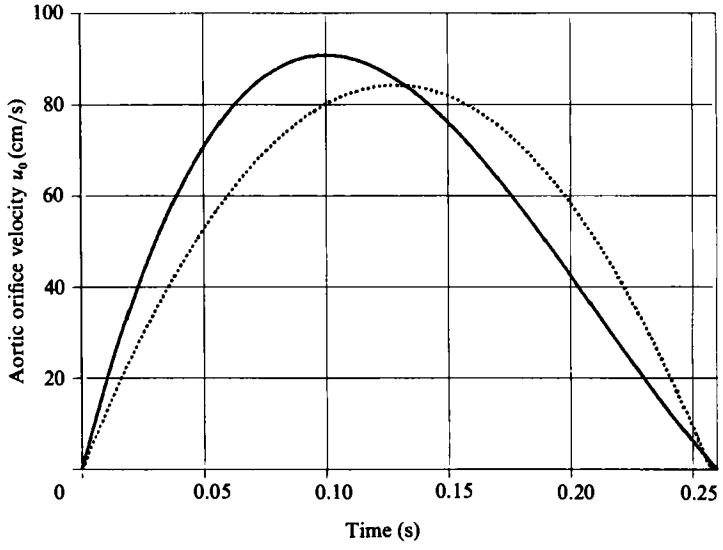

FIGURE 3. Time-dependent aortic orifice velocity: ——, natural conditions; · · · · ·, a quadratic function of time for the purpose of comparison with experiments.

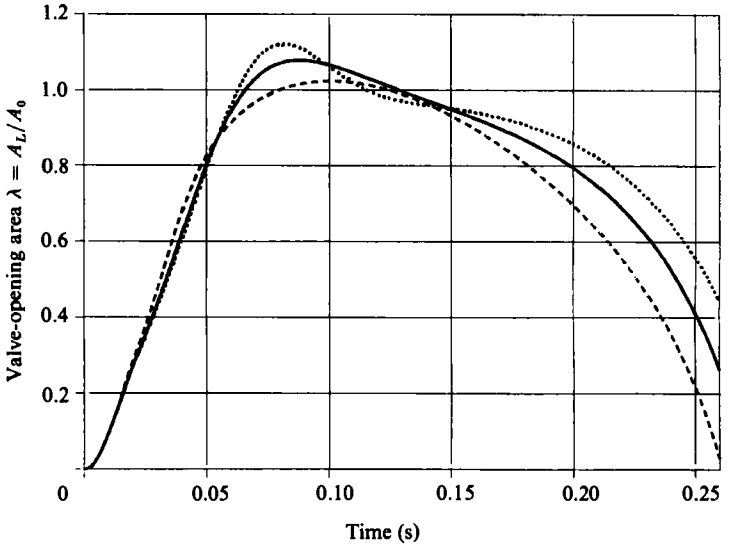

FIGURE 4. Time-dependent aortic-valve motion for different sizes of the sinus of Valsalva: ——, $m = 1.\bar{6}$, natural size; – – –, $m \to \infty$, size approaching infinity; · · · · ·, $m = 0.8\bar{3}$, half the natural size.

In figure 5 the theoretical result (solid curve) is compared with experimental data (○) obtained by Bellhouse & Talbot (1969) in experiments with a symmetric pulsatile flow as shown in figure 3 (dotted curve). With a peak velocity $u_{0\,\max} = 85.1$ cm/s of such a pulsatile flow ($T = 260$ s) the stroke volume remains unchanged ($V = 5$ l min^{-1}) using the same valve as in the preceding sections.

The agreement is only moderate. However, one should bear in mind that the experimental data contain some uncertainties too; for instance, in the experiment the edges of the cusps are invisible for $\lambda > 1$.

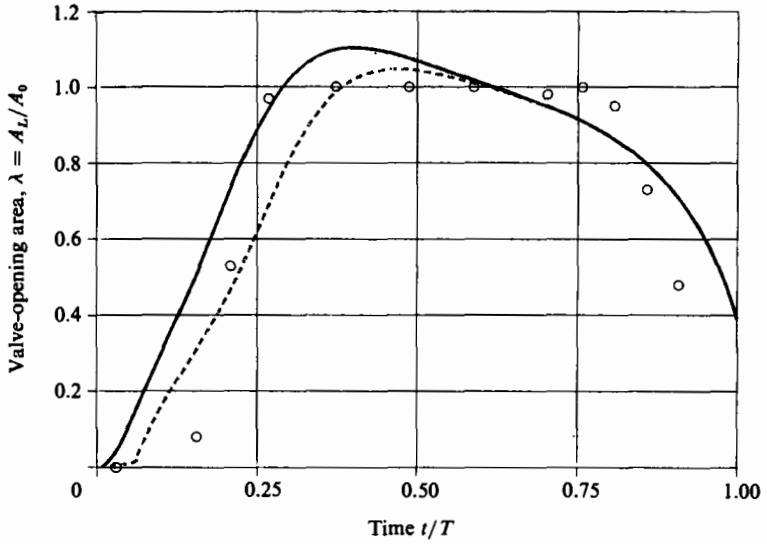

FIGURE 5. Time-dependent aortic-valve motion: ⊙, data obtained from the Bellhouse & Talbot (1969) experiment; ——, motion computed by the present theoretical model (pulsatile flow with parabolic velocity variation as in figure 3, $T = 260$ ms); - - - - -, result of the same model but with a delayed starting time.

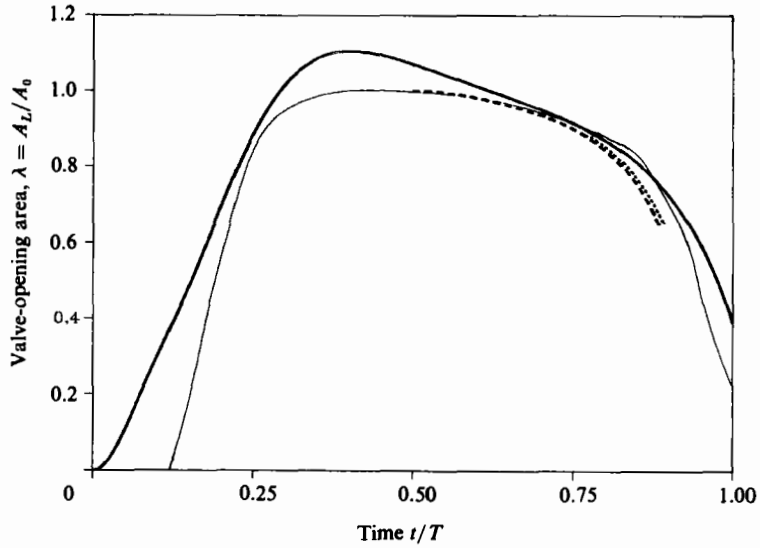

FIGURE 6. Time-dependent aortic-valve motion, a comparison with the results of other authors (pulsatile flow with parabolic velocity variation as in figure 3, $T = 260$ ms): ——, present theoretical model; ——, Lee & Talbot (1979); – – –, van Steenhoven & van Dongen (1979); · · · · ·, Peskin (1982).

The broken curve in figure 5 represents the same theoretical result, but the starting time t_s is somewhat delayed ($t_s/T = 0.05$); the agreement with experimental data is slightly better. At the very beginning of valve opening the cusps in a natural valve are bulged forward, but the valve remains closed for this short time interval, only thereafter do the cusps move rapidly to their fully open position, offering no resistance to forward flow. That of course is not true for the model valve, the cusps of which are rigid and move forward immediately when ejection begins.

In the case of a valve opening with a delayed starting time the initial conditions $\lambda = 0$, $\mathrm{d}^2\lambda/\mathrm{d}t^2 = 0$ at $t = t_s$ have been used instead of (23).

A comparison with the theoretical results of other authors is shown in figure 6. The heavy solid curve again represents the valve motion computed by the present theory in the case of an orifice flow $u_0(t)$ having a parabolic variation with time. The thin solid curve shows the result of Lee & Talbot (1979) using the assumption $p_a(x, t) = p_i(x_L, t)$ for the pressure at the sinus side of the cusp; this corresponds to the case $m \to \infty$ in the present model, i.e. an unlimited sinus of Valsalva. These authors compute the valve motion with a delayed starting time t_s in order to improve the agreement with experimental data; however, this is not justified for a model with rigid cusps.

The two other curves are the results of integrating the equations obtained by van Steenhoven & van Dongen (1979) (dotted curve) and Peskin (1982) (broken curve); see table 2.

7. Concluding remarks

The one-dimensionality of the valve model used in the present paper prohibits the formation of a trapped vortex in the aortic sinuses. Nevertheless, a correctly functioning closure can be computed in accordance with experimental data. Obviously such a vortex – appearing in the physiological valve – does not play an essential role in controlling the closure of the valve. The flow deceleration is solely responsible for valve closure.

This, of course, does not mean there is no vortex acting on the cusp. Even in this one-dimensional model there is still a 'hidden' vortex (Peskin 1982) – a vortex sheet localized on the valve leaflet due to the different tangential velocities on the two sides of the leaflet.

The trapped vortices in the sinuses may be unimportant for the closing of the valve, but they are not unnecessary; rather they have other important functions, such as preventing projection of the cusps too far into the sinus cavities and protecting the ostia of the coronary arteries from being occluded; at peak systole the cusps are possibly balanced between the sinus vortex and the aortic flow. In addition, sinus vortices may prevent stagnation of blood and thrombus deposition behind the cusps.

The author would particularly like to thank Dr G. Gross for his considerable assistance in carrying out the numerical integrations of $(22a, b)$. He is also deeply indebted to his late colleague Professor E. Becker, with whom he had several very helpful discussions on the topic of this paper.

REFERENCES

Bellhouse, B. J. 1969 Velocity and pressure distributions in the aortic valve. *J. Fluid Mech.* **37**, 587.

Bellhouse, B. J. 1972 Fluid mechanics of a model mitral valve and left ventricle. *Cardiovasc. Res.* **6**, 199.

Bellhouse, B. J. 1980 Fluid mechanics of the aortic valve. In *Cardiac Dynamics* (ed. Baan, Arntzenius & Yellin), chap. 6.4, p. 489. Nijhoff.

Bellhouse, B. J. & Talbot, L. 1969 The fluid mechanics of the aortic valve. *J. Fluid Mech.* **35**, 721.

Davila, J. C. 1961 The mechanics of cardiac valves. In *Prosthetic Valves for Cardiac Surgery* (ed. K. A. Merendino). C. C. Thomas, Springfield, Ill.

GILLANI, N. V. & SWANSON, W. M. 1976 Time-dependent laminar incompressible flow through a spherical cavity. *J. Fluid Mech.* **78**, 99.

HENDERSON, Y. & JOHNSON, F. E. 1912 Two modes of closure of the heart valves. *Heart* **4**, 69.

HUNG, T.-K. & SCHUESSLER, G. B. 1977 An analysis of the hemodynamics of the opening of aortic valves. *J. Biomech.* **10**, 597.

HWANG, N. H. C. 1977 Flow dynamics of natural valves in the left heart. In *Cardiovascular Flow Dynamics and Measurements* (ed. N. H. C. Hwang & N. A. Norman), chap. 21, p. 825. University Park Press, Baltimore.

LEE, C. S. F. & TALBOT, L. 1979 A fluid mechanical study of the closure of heart valves. *J. Fluid Mech.* **91**, 41.

LEONARDO DA VINCI 1513 *Quaderni d'Anatomica* **2**, 9.

MCCRACKEN, M. F. & PESKIN, C. S. 1980 A vortex method for blood flow through heart valves. *J. Comp. Phys.* **35**, 183.

PESKIN, C. S. 1972 Flow patterns around heart valves: a numerical method. *J. Comp. Phys.* **10**, 252.

PESKIN, C. S. 1982 The fluid dynamics of heart valves: experimental, theoretical and computational methods. *Ann. Rev. Fluid Mech.* **14**, 235.

SWANSON, W. M. & CLARK, R. E. 1974 Dimensions and geometric relationships in the human aortic valve as a function of pressure. *Circ. Res.* **35**, 871.

VALSALVA, A. M. 1740 *Opera Postuma*, Venice (in Latin).

VAN STEENHOVEN, A. A. & VAN DONGEN, M. E. H. 1979 Model studies of the closing behaviour of the aortic valve. *J. Fluid Mech.* **90**, 21.

VAN STEENHOVEN, A. A., VERLAN, C. W. J., VEENSTRA, P. C. & RENEMAN, R. S. 1980 The closing behaviour of the aortic valve. In *Cardiac Dynamics* (ed. Baan, Arntzenius & Yellin), chap. 6.3, p. 477. Nijhoff.